10th IMC
10th International Masonry Conference
G. Milani, A. Taliercio and S. Garrity (eds.)
Milan, Italy, July 9-11, 2018

THE IMPORTANCE OF MODELLING ASSUMPTIONS WHEN ANALYSING THE DYNAMIC RESPONSE OF A MASONRY RAILWAY VIADUCT

Sam H. Cocking[1], Sinan Acikgoz[1,2], and Matthew J. DeJong[1]

[1] Department of Engineering, University of Cambridge, Cambridge (UK)
e-mail: {sc740, msa44, mjd97}@cam.ac.uk

[2] Centre for Smart Infrastructure and Construction, University of Cambridge, Cambridge (UK)

Keywords: Arch Viaduct; Monitoring; Computational Modelling; Historic Masonry.

Abstract. *The masonry viaduct at Marsh Lane is an important part of the railway network near Leeds, UK, dating from the 1860s. However, deterioration has resulted in notable deflections under train loads, which have concerned asset managers. Coupled with uncertainty regarding the true structural behaviour under serviceability conditions, this has led to detailed monitoring of the viaduct. This paper summarises the main conclusions of the monitoring installation before focusing on the evaluation of computational modelling of the viaduct, through comparison of modelling and monitoring results. In the monitoring scheme, fibre-optic cables containing Fibre-Bragg Gratings allowed measurement of dynamic in-plane barrel strains while digital image correlation captured displacements using commercial video cameras. The results illuminated a complicated three-dimensional dynamic response under train loading and highlighted the importance of interaction between adjacent spans. Separately, rail loading of the viaduct was simulated with a series of finite element models, each with increasing levels of complexity, to establish the relative stiffness contributions of various structural components. These models were then compared to detailed measurements from the real viaduct so that their validity could be evaluated. This approach revealed the impact of some common modelling assumptions and permitted assessment of nonlinear contributions to structural behaviour.*

1 INTRODUCTION

Masonry arch bridges and viaducts form a key component of the railway network in the UK and other European countries. Many of these structures are now approaching 150 years old and are still in active service, carrying passenger or freight trains. They may show signs of distress such as cracking or liveliness under load, but since their serviceability behaviour is often complex it can be unclear whether such signs are a cause for concern. Greater understanding of this behaviour is therefore necessary to allow repair and maintenance work to be prioritised across the network and tailored to the conditions of individual bridges.

Researchers and consultants may choose to use a finite element (FE) model to investigate the behaviour of a masonry arch bridge. To create an accurate representation of the structure requires that the model include the nonlinear behaviour of masonry. It is also necessary to have knowledge of the geometry and material properties of all structural components; some of these such as the backing and foundations are hidden and therefore difficult to assess. Furthermore, soil-structure interaction will play a part in the response and consequently the soil properties should be established. These properties will vary spatially, while often a computational model will use only average values. Because of this, the resulting finite element model can be complex and time intensive to construct and run. Moreover, it will remain sensitive to input parameters which are typically uncertain. A sensitivity analysis can consider likely ranges of these parameters, but this adds yet more expense. Even if this approach can be justified by a researcher or consultant in some unique cases, it is impractical for practicing asset engineers to adopt it for all the structures in their care.

Often, asset engineers will use limit state software when assessing their bridges. These consider the ultimate limit state (ULS) of the bridge when it is on the point of collapse, and the loads required to achieve this are compared against the real loads currently acting on the structure. Input uncertainties will remain in the limit state approach and so either average values of unknown properties will be used, or safe ranges chosen which result in a range of potential ULS loads against which current working loads are assessed. However, this approach reveals little about what the behaviour of the bridge *should* be under its working loads; investigating this may well be a better approach for assessing the severity of any damage.

Therefore, it is important to consider what can be gleaned from a simplified analysis, performed under service conditions. This paper addresses this question, using the case study of the Marsh Lane viaduct in the UK and evaluating monitoring data of this structure's serviceability response against a baseline given by simplified linear elastic FE analysis.

2 MARSH LANE VIADUCT

The Marsh Lane viaduct is located in Leeds, UK, and was constructed in the 1860s. It has suffered extensive cracking and water damage throughout its life, as well as permanent deformations resulting from the spreading of relieving arches in the piers. Monitoring of the viaduct, which was carried out by the Cambridge Centre for Smart Infrastructure and Construction (CSIC), was commissioned in response to visible live load deflections which concerned the asset managers. Figure 1 shows a photograph of the monitored spans of the viaduct, while key dimensions are indicated in Figure 2.

The most substantial forms of damage include longitudinal cracks springing from above relieving arches in the piers, which continue along the centreline of the main arch soffits. In addition to these, there are transverse cracks in the arch soffits, just above the vertical level of internal rigid backing. Large regions of the soffits are also depressed, due to long-term deformations of the as-built geometry.

Figure 1: The Marsh Lane viaduct.

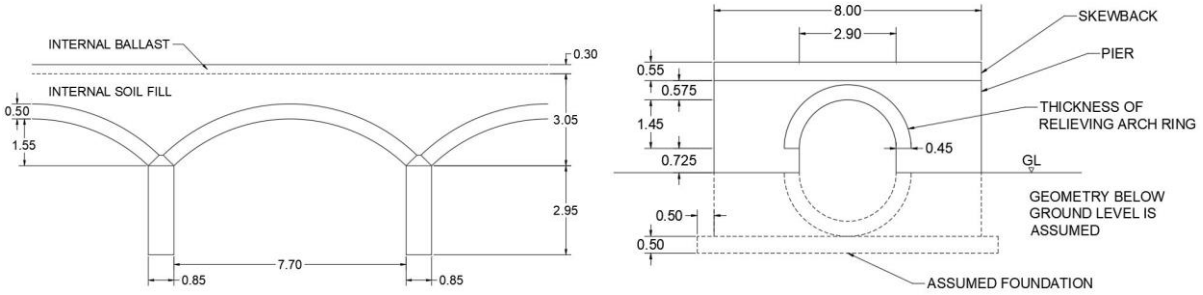

(a) (b)

Figure 2: (a) main span elevation, viewed along the global transverse direction, and (b) pier elevation, viewed along the global longitudinal direction, views of Marsh Lane viaduct (with key dimensions in metres).

3 MONITORING SCHEME

Monitoring data was collected at Marsh Lane viaduct on two occasions in 2016. The installation scheme is described in full detail in a paper by Acikgoz et al [1]. The key technologies used were fibre-optic Fibre-Bragg Gratings (FBGs) to measure in-plane strains and digital image correlation to capture displacements and any rigid body rotations.

Further monitoring work is currently underway to evaluate degradation and temperature-related changes in the response, but this paper considers only data from the initial monitoring campaign.

3.1 FBG installation

In-plane barrel strains were measured using Fibre-Bragg Gratings, which are point sensors embedded into a fibre-optic cable of arbitrary length. Several cables instrumented in this fashion were strung across the structure and clamped in places of interest such that the individual FBGs measured average dynamic strains across gauge lengths given by the distances between clamps. One end of each cable was connected to an analyser, which sent pulses of light along the cables and examined the backscattered light for any shifts in each of the FBGs' unique Bragg wavelengths, which could then be related to the strains experienced by these sensors.

Of particular interest in this paper are the longitudinal cables which were positioned on the arch soffits running directly underneath the two track centrelines of the viaduct. Figure 3 shows the locations of FBGs on these four longitudinal monitoring cables L1 to L4, as seen when looking up from ground level. Points S1 to S8 are the eight locations on each cable

where local in-plane strains were measured in the arch barrels. Here, the notation is such that sensor S1 is the first to be passed by a train as it travels on the track above, while S8 is the last.

The span opening response was also measured by FBGs, positioned between the skew-backs at the tops of the piers in each of the longitudinal planes L1 to L4. These strains were post-processed to give pier-to-pier opening displacements. Figure 4 shows a typical pier-to-pier measurement as a train passes over the viaduct.

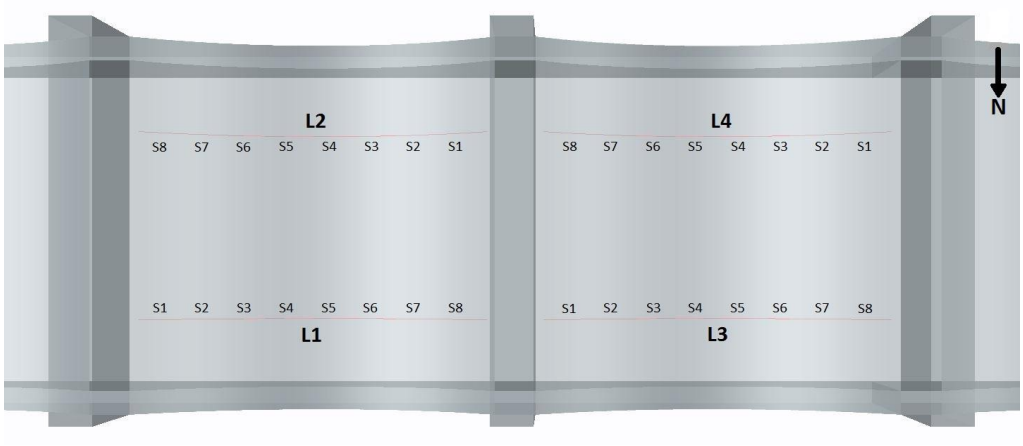

Figure 3: The four longitudinal monitoring cables L1 to L4, with sensor locations S1 to S8 shown for each cable.

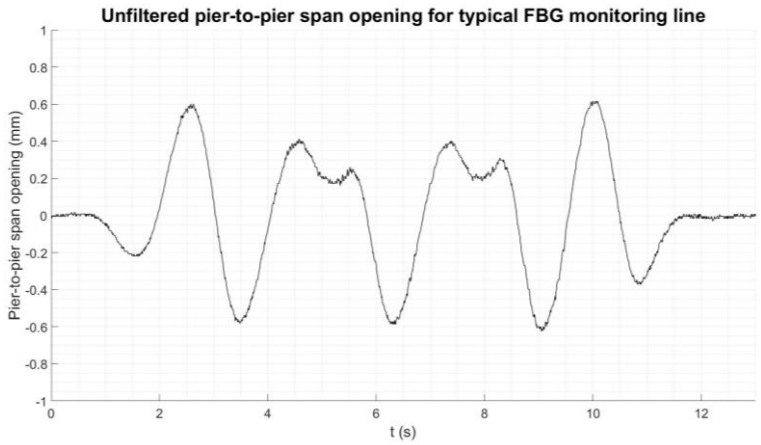

Figure 4: Typical measured pier-to-pier response as a train passes on the track above.

3.2 Digital image correlation

While the FBG installation is well-suited to monitoring in-plane strains, it was also desired to measure displacements, such as the crown vertical displacement. This was achieved using the Imetrum videogrammetry system. While the FBG scheme was custom-made for this project, the Imetrum equipment is a commercially available product [2].

In order to achieve high quality displacement data, it was necessary to have highly textured patterns to track. Although the natural texture of brickwork and mortar can be used for video measurements, high-contrast artificial targets were also printed and attached to the structure in some locations. A view of one arch soffit showing these targets is given in Figure 5.

Typical crown vertical displacement is indicated later in this paper in Figure 9.

Figure 5: Examples of the videogrammetry targets used at Marsh Lane viaduct.

3.3 Monitoring conclusions

Monitoring of the Marsh Lane viaduct revealed a pseudo-static and three-dimensional mode of response under the action of live loads. This is discussed in detail by Acikgoz et al [1] and is most simply described by considering response components in the global longitudinal and transverse directions.

Considering the longitudinal plane of the viaduct, the application of vertical axle loads from a passing train leads to spreading of the arch directly beneath the axle, while the two spans immediately adjacent contract. This contraction is possible because the carriage lengths are approximately double the span length. As such, when an axle is positioned near the crown of one span, no loads are applied to the two adjacent spans. This results in a cycle of pier-to-pier span opening and closing as the multi-carriage train passes overhead, with accompanying rotation of the piers below. This cycle can be clearly seen in the monitoring data in Figure 4.

The deformation of the spans is limited somewhat by the solid backing over the arch haunches, which itself rotates as a rigid body. Due to pre-existing damage, connectivity between this rigid backing and arch barrels is strong in compression but negligible in tension, and so the rotation of this backing has an impact on the mode of deformation of the arch barrels.

The transverse component of the response mode is best visualised by considering a single pier and its central relieving arch, along with the skewback and main arch haunches above. The transverse response involves spreading of the relieving arch in time with opening of the longitudinal cracks in the main arch soffit above. The two sides of the pier and two regions of the main arch, either side of the longitudinal crack, can be considered as four macro blocks. Spreading of the relieving arch causes outward rotation of the two pier macro blocks. This rotation only maintains connectivity between the pier blocks and the skewback, which moves with the main arch blocks, over the central portion of the pier, close to the relieving arch. However, towards the outer edges of the pier there will be separation between the pier and the skewback. When the pier is viewed edge-on, this allows the pier and skewback to appear to move independently. This provides an explanation for the phenomenon sometimes referred to as “skewback rocking,” which has been noted by other engineers [3].

4 FINITE ELEMENT MODELLING SCHEME

4.1 Model overview

A series of linear elastic finite element models were constructed of the Marsh Lane viaduct, using Abaqus FEA software. Starting from a basic model of the piers and main arches, increasing amounts of structure were added in each subsequent model in order to gauge the relative importance of the individual structural components. These were either modelled explicitly with new finite elements, as in the case of shell elements for the piers, arches, and the spandrel walls, or using idealised boundary conditions as was done for the rigid backing. This backing was modelled as a series of rigid ties across the arch haunches.

From a sensitivity study it was concluded that it was only necessary to model five spans of the viaduct in order that the behaviour of the central span would not be influenced by the boundary conditions applied to the outermost spans. Therefore, in all cases presented here, five spans were modelled, and the results of the central span were analysed.

The finite element models are summarised in Table 1 and shown in Figure 6. It was necessary to make assumptions regarding the geometry and properties of the viaduct, when assembling these models. Some assumptions could be verified; for example, the vertical level of rigid backing was not visible but could be inferred from local spalling on the arch intrados, which reliably occurred at this level due to the step change in stiffness that comes from moving from rigid (solid) backing into soil backfill with a much lower Young's Modulus. However, other assumptions could not be verified. These include the hidden geometry of the foundations, for which no record drawings existed. These were modelled based on guidance from Network Rail, the asset owners, regarding conventional foundations for that time period and structural typology.

The most critical assumptions regarded the Young's Moduli of the masonry and soil, which unfortunately could not be confirmed by site tests. Again, conventional values from the literature were used, based on a qualitative assessment of the masonry and soil conditions [4, 5]. The soil properties were then used to estimate the stiffnesses of soil springs, in order to account for soil-structure interaction in the FE models. The assumed values of these properties and the resulting soil spring stiffnesses are given in Table 2. The vertical soil spring stiffness was refined from its initial calculated value, using deflection data captured during monitoring at a point when a train axle was positioned directly above one of the viaduct piers. It is the refined value that is presented in Table 2.

FE Model	Description
1	Basic model containing main arches, piers, and soil springs
2	Model 1, with inclusion of spandrel walls
3	Model 2, with inclusion of rigid backing
4	Model 3, with inclusion of relieving arches

Table 1: Overview of the four finite element models of Marsh Lane viaduct.

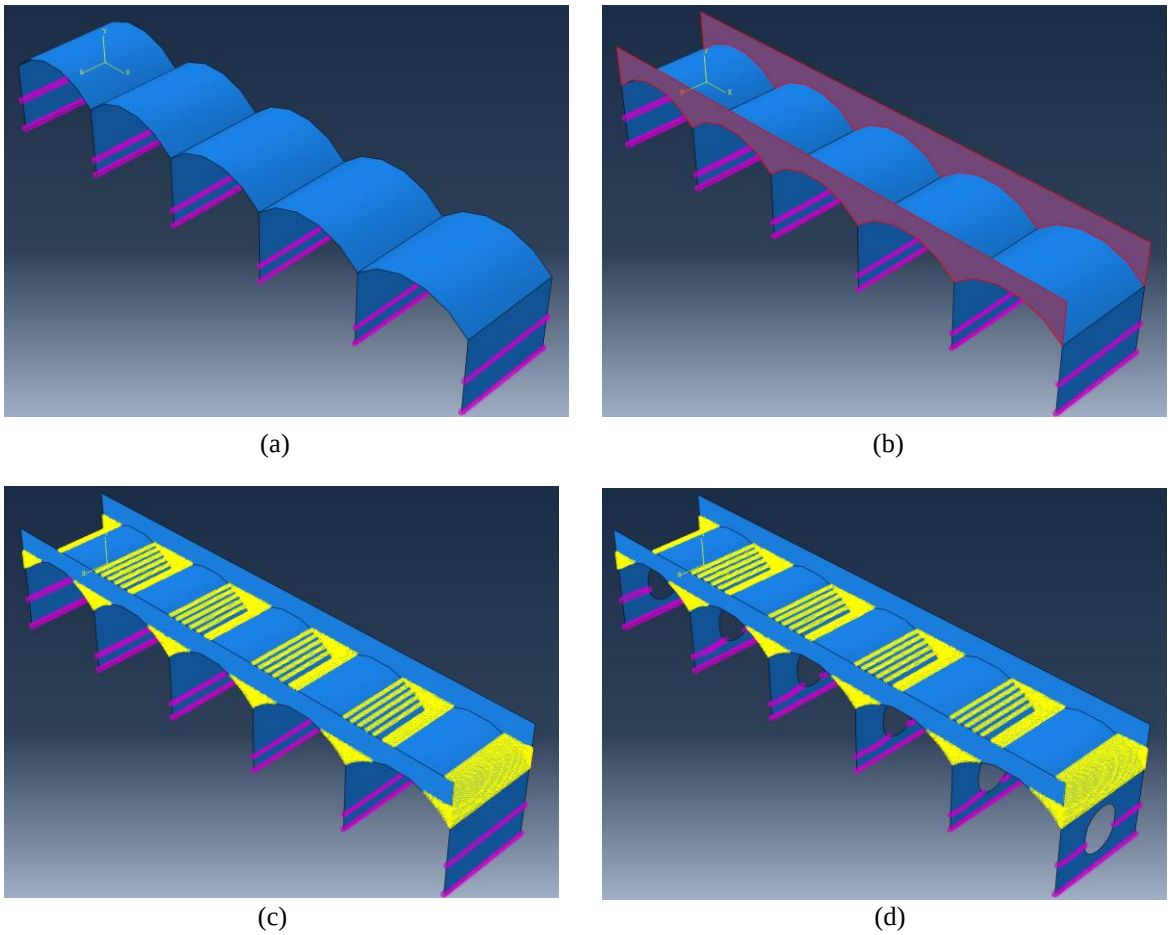

(a) (b)

(c) (d)

Figure 6: Views of the four finite element models of Marsh Lane viaduct: (a) Model 1, (b) Model 2, (c) Model 3 and (d) Model 4.

Parameter	Value
Young's modulus of masonry, $E_{masonry}$	5 GPa
Poisson's ratio of masonry, $\nu_{masonry}$	0.2
Density of masonry, $\rho_{masonry}$	1600 kg/m^3
Young's modulus of soil, E_{soil}	250 kPa
Poisson's ratio of soil, ν_{soil}	0.3
Soil vertical translational spring, K_v	984x10^6 N/m
Soil longitudinal translational spring, K_h	2.30x10^6 N/m
Soil rotational spring, K_r	12.5x10^6 Nm

Table 2: Assumed values of material properties and resulting soil spring stiffnesses.

Wolf's equations were used for the soil spring stiffness calculations; these are simplified, empirical equations for embedded foundations and are presented below as equations (1) to (3). Along with other sources, Wolf's equations were incorporated into the more complex and better-known equations proposed by Gazetas [6].

$$K_r = \frac{Gb^3}{1-\nu}\left[3.73\left(\frac{l}{b}\right)^{2.4} + 0.27\right]\left[1 + \frac{e}{b} + \frac{1.6}{0.35 + \left(\frac{l}{b}\right)^4}\left(\frac{e}{b}\right)^2\right] \quad (1)$$

$$K_h = \frac{Gb}{2-\nu}\left[6.8\left(\frac{l}{b}\right)^{0.65} + 2.4\right]\left[1 + \left(0.33 + \frac{1.34}{1 + \frac{l}{b}}\right)\left(\frac{e}{b}\right)^{0.8}\right] \quad (2)$$

$$K_v = \frac{Gb}{2-\nu}\left[3.1\left(\frac{l}{b}\right)^{0.75} + 1.6\right]\left[1 + \left(0.25 + \frac{0.25b}{l}\right)\left(\frac{e}{b}\right)^{0.8}\right] \quad (3)$$

In Wolf's equations, G is the shear modulus, ν is the Poisson's ratio, $2b$ is the foundation length, $2l$ is its width and e is its embedment depth.

4.2 Application of loading

Since the ballast and fill were not included in the FE models, it was necessary to perform initial calculations to determine the distribution of live loads through these materials. Starting from axle loads applied to the rails, distribution angles of 15° and 30° were assumed for the ballast and fill respectively. Patch loads were thus obtained, and these were applied directly to the arch extrados in the FE model.

Since the monitoring data indicated that the response of the viaduct was pseudo-static [1], it was deemed sufficient to perform static FE calculations. To simplify computation, nine analysis steps were identified based on the salient points of the pier-to-pier response of Figure 4. These nine points are shown on a typical smoothed pier-to-pier response in Figure 7, along with the corresponding axle locations at these times. Due to the interaction effect between spans, three spans are considered. Patch loads were calculated for each of these steps and applied to the FE models.

In Figure 7, the axle loads correspond to a train that is travelling from left to right. Steps 1 to 3 only include the leading axle of the train, though by symmetry they can also represent the rear axle. In steps 4 to 6, both axle loads from a single carriage are acting on the three spans. It is significant that the distance between these axles is approximately double the span length; this gives rise to the worst-case response of the viaduct. Lastly, in steps 7 to 9, the rear axle of one carriage interacts with the leading axle of the carriage behind it. This results in a double peak in the response.

Between these modelling steps, behaviour is assumed to follow the pattern that is observed in the smoothed measured response. In Figures 8 and 9, these regions are filled in using a spline function so that the trends can be compared against monitoring results. Numerical comparisons, however, are only made using results from the nine modelling steps.

In Figure 10, which examines in-plane strains across the arch barrel, results from the nine modelling steps are plotted without any interpolation. This is because the patterns of the in-plane strain and pier-to-pier responses are in some cases significantly different and meaningful interpolation is therefore no longer possible using only data taken at these modelling steps. Instead, it is more informative to compare the point values.

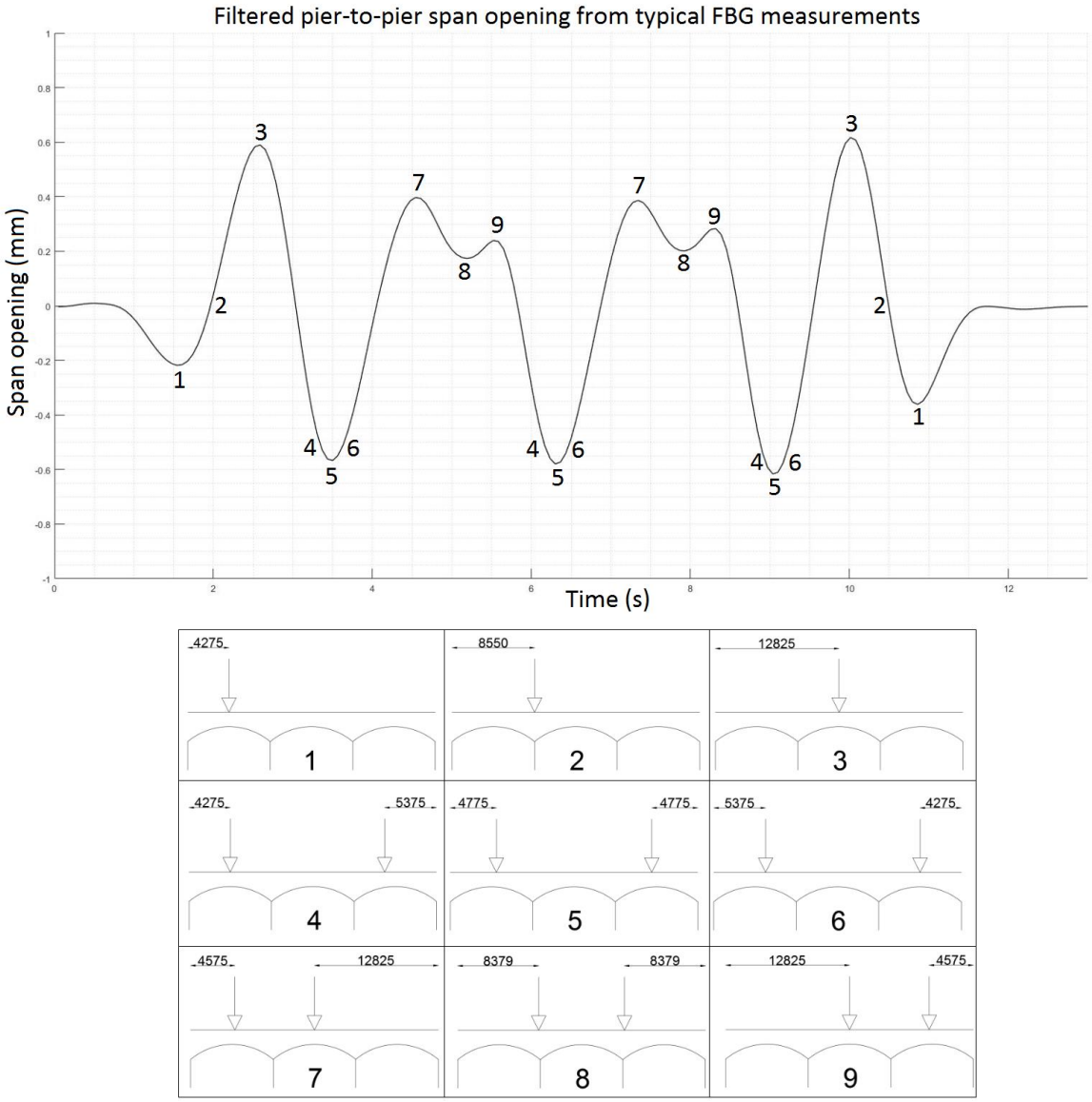

Figure 7: Filtered pier-to-pier response indicating the nine points chosen as modelling steps for the FE analysis, and corresponding locations of axle loads for each step (with dimensions in millimetres).

4.3 Boundary conditions and restraints

In each of the FE models, only five spans of the viaduct were considered. Boundary conditions were applied to the outer edges of the first and fifth span. These prevented longitudinal translation of the outer piers, longitudinal translation and rotation of the outer edges of the spandrel walls, and vertical translation of the outer arch springings. Transverse translation was only restrained at the central points of each pier base, to avoid over-constraining the model.

Soil springs were applied to all but the outer piers, which were more fully restrained. The rotational and vertical translational springs were applied directly to the pier bases, while the longitudinal translational springs were applied at a level coinciding with the mid-depth of the embedded region of the piers. Although single values of the spring constants were calculated, as shown in Table 2, in the FE models these were distributed across the widths of the piers.

5 COMPARISON OF MONITORING DATA WITH FINITE ELEMENT BASELINE

A fully accurate linear elastic FE model, which captures all important structural components and interaction effects between components, and which uses the correct input values of properties such as the Young's modulus, would theoretically represent the undamaged condition of the true viaduct as long as loads remain sufficiently low. In other words, in terms of the response characteristics such as the pier-to-pier span opening displacement, such a model would produce results which would be matched by the real structure, while it remains undamaged, but which will be exceeded once the structure experiences damage. This is due to stiffness losses that result from the damage.

Furthermore, nonlinear behaviour as a result of this damage might reasonably be expected to change the "pattern" of response characteristics, so that a graph of a given characteristic against time would have a different shape to an analogous graph from a point when there was no damage, and the system remained elastic. Therefore, even if the magnitude of the response is not known, for example because there is uncertainty regarding the material properties, it is informative to compare the measured response "pattern" against the baseline of the linear elastic FE analysis, as this can reveal whether damage has been extensive enough to result in notable changes in behaviour.

There are two categories of response characteristic that can be investigated. "Global" response parameters indicate the behaviour of the arch overall; these include the pier-to-pier span opening or the crown vertical displacement. Meanwhile, an example of "local" response parameters would be the variation of strain at points throughout the arch barrel; a greater number of local parameters are needed to give a full view of the arch behaviour, but they also provide more detail as a result.

It is worth noting that, in current UK practice, single (point) measurements are preferred by asset managers; in particular the crown vertical displacement tends to be used. This is because of the practicalities involved in monitoring a very large number of structures. It is still possible to track the condition of an asset over time by repeatedly taking this one type of measurement; it is expected that any deterioration which might require further action also tends to cause an increase in the global response parameter. However, any precise changes to the mode of response which may have resulted from the (case-specific) damage cannot be known without considering local response parameters.

5.1 "Global" response parameters

Figure 8 compares the pier-to-pier span opening response of all four FE models with the observed response of the real viaduct in its current condition, as captured by FBG sensors. From this plot, it is clear that modelling all key structural components is important in order for computational results to approach the monitoring data; this is discussed further in the following section.

Figure 9, meanwhile, compares the crown vertical displacement and crown in-plane strain for the final FE model and the real viaduct. Vertical displacements were captured using videogrammetry while the crown strain was once again measured using fibre-optic FBGs.

In all cases, it seems that the patterns of the responses are consistent between the FE models and the monitoring data. The addition of components such as the spandrel walls and rigid backing above the arch haunches does not significantly change the patterns either. In the case of the spandrel walls, this can be explained by considering that the inclusion of spandrels should not change the mode of response of a longitudinal "slice" of the arch sufficiently far from the spandrel itself, other than causing a substantial increase in stiffness. The main effect

of the spandrels, while they remain fully connected to the arch barrel, is observed in the transverse response of the viaduct and in particular in transverse flexure of the barrel. Because the response characteristics considered here were measured purely in the longitudinal plane, the spandrels had little impact on the pattern of this response, though they reduced the magnitude of response significantly.

As for the rigid backing, this does locally affect the response of the arch haunches. This is seen in local strain data for this region and discussed in section 5.3. However, the parameters considered here are either measured between the skewbacks or at the arch crown, which are locations sufficiently separated from the arch haunches for any influence to be exerted by the backing. Again, it is a stiffness increase that is seen as the primary impact of the rigid backing on these global response parameters.

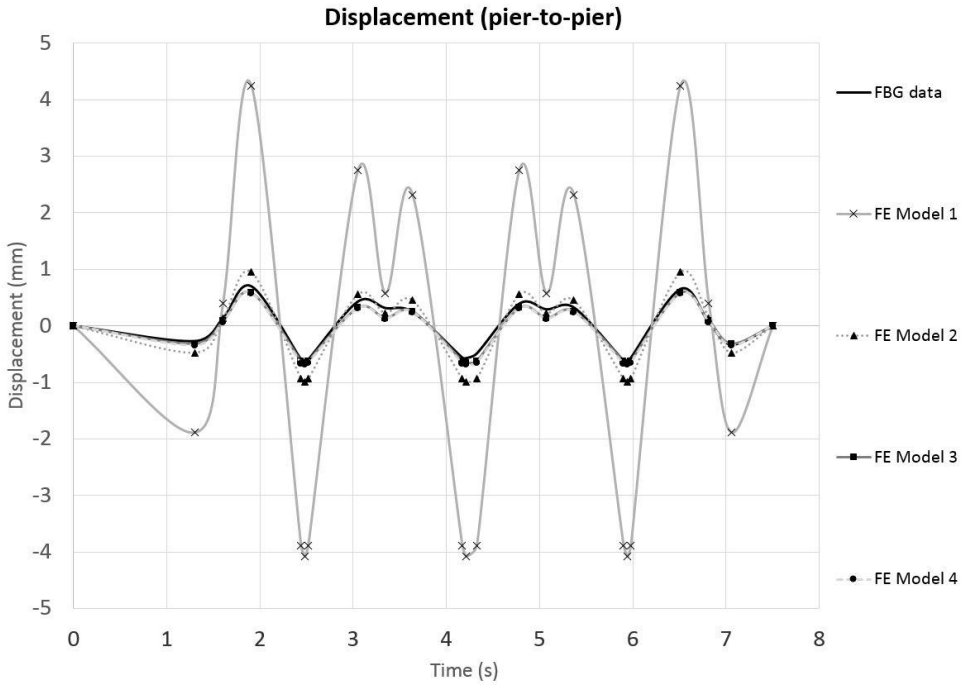

Figure 8: Pier-to-pier opening responses of the four FE models and the real viaduct.

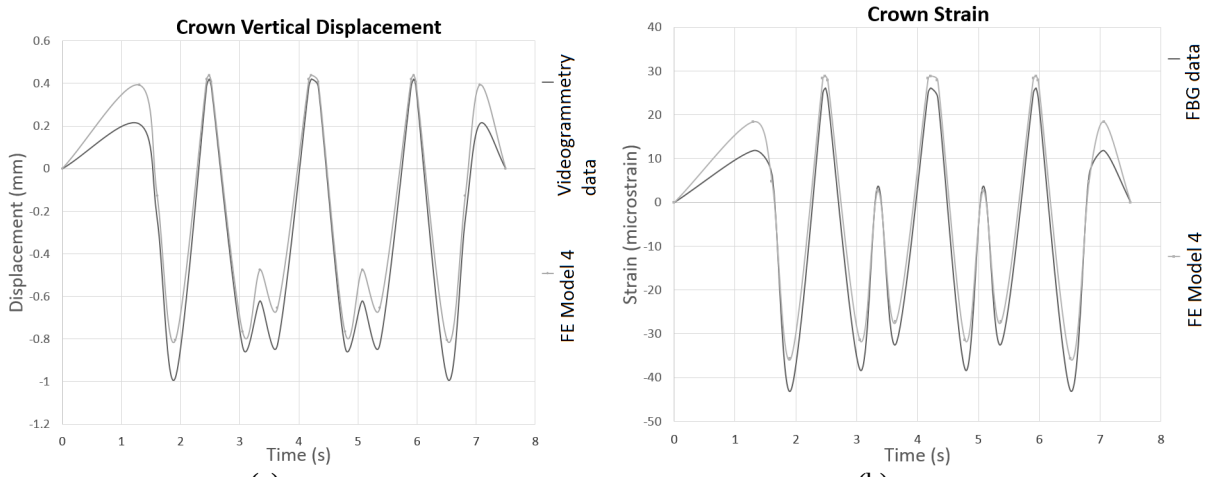

(a) (b)

Figure 9: (a) crown vertical displacement and (b) crown in-plane strain of the final FE model and the real viaduct.

5.2 Relative contributions to global structural performance

It was also possible to investigate the relative stiffness contributions of the viaduct's various structural components in this finite element survey. The series of models, as detailed in Table 1, were constructed so that each included a further structural element, until all key components had been modelled. The magnitude of global response parameters was compared before and after the addition of new structural components. By setting the final model at a level of 100% effectiveness in capturing live load deflections, the difference between each pair of models then corresponded to the relative importance of the component that was added in that modelling step.

It is worth noting that possible uncertainties in the input parameters are of less concern in this case than they were when comparing the results of FE analysis to monitoring data. Since the models are linear elastic, each one should be equally affected by any variations of the input parameters. Therefore, the ratios of output should remain the same.

The relative contributions of the various structural components are presented below in Table 3 and can be visualised by comparing the tabulated values with Figure 8. In particular, the large impact of including spandrel walls in the model is clear in Figure 8. This is noteworthy, since often a two-dimensional analysis of a masonry arch bridge might neglect the spandrel walls and arch-backing interaction. The importance of these features is already established in increasing the ultimate load of bridges [7-9] and these results demonstrate that the effect is also present in serviceability conditions. In all cases except for total spandrel wall separation, this effect is worth bearing in mind.

The "relative effectiveness" observed in the real response of the viaduct is also presented in Table 3. This suggests that the current behaviour, even if it has alarmed asset managers, corresponds to only a small reduction in performance from the original, undamaged condition. This must be treated with caution, however, due to the uncertainties remaining in some input parameters. Of most importance here are the soil and masonry Young's moduli but there are also the soil-structure interaction effects, where Wolf's equations have been used in conjunction with assumed geometry below ground level.

Model type	Model 1	Model 2	Model 3	Model 4	The real viaduct
New structural component	Piers, arches, and soil springs	Spandrel walls	Rigid backing above arch haunches	Relieving arches (in piers)	N/A
Additional contribution to global resistance	13%	48%	39%	0%	N/A
Total contribution to global resistance	13%	61%	100%	100%	91%

Table 3: Relative contributions of structural components to the resistance of live load deflections.

The values of Young's moduli which have been used here were chosen on the basis of qualitative assessment of the local conditions and safe ranges of possible values, from the literature [4, 5]. The highest values from safe ranges were chosen, corresponding to values towards the upper limit of the possible stiffness. When it is considered that reducing the stiffness will increase the magnitude of live load deflections and that the results of the final

FE model are already quite close to the monitored response, which physically cannot be exceeded by a linear elastic model purporting to show the undamaged response, then it seems reasonably likely that the true stiffnesses are not far from the assumed values.

On the other hand, while Network Rail guidance on common practice has been applied in calculations of the soil-structure interaction, uncertainties here could lead to either increases or decreases in the model response. Indeed, when the calculated vertical spring stiffness was recalibrated based on observations made during monitoring, it was found that the new value corresponded to a substantial increase in stiffness. If the other soil springs have been similarly underestimated, which remains unclear, then a lower value of Young's modulus could be accommodated in the masonry without giving rise to unphysical results. Equally, if the soil springs should in fact be stiffer but the masonry Young's modulus has been accurately predicted, then the resulting FE model would yield output of reduced magnitude. Viewed through this lens, the true structure would appear to have suffered more significant damage than Table 3 suggests.

5.3 "Local" response parameters

The local strain distribution over the arch barrel, at points S1 to S8, is shown in Figure 10. Results are presented for the final FE model and four sets of FBG data. These datasets show the response along all four longitudinal cables, L1 to L4, on both sides of the two spans which were monitored.

The variation between FBG datasets indicates the different levels of local damage in the vicinity of each cable. The most notable damage is the transverse cracks, which cause much larger strains at points S2 on cable L1 and S7 on cable L3. Another transverse crack can be seen at point S8 of cable L2, although this is less severe.

Leaving aside the locations of severe damage, it can be seen that the comparison of local strain data between the final FE model and the monitoring data is more favourable closer to the centre of the arch than it is near the haunches. In particular, points S4 and S5, which are either side of the crown, agree well. Further away from the crown the comparison is less convincing and there are several reasons why this might be the case.

Firstly, while the arch is in reasonably good condition near the crown there is evidence of damage closer to the haunches, including but not limited to the cracks described above. Numerous other, minor cracks also exist in the soffit. Close to the haunches, some regions of the soffit are also depressed as a result of spreading of the relieving arches in the piers.

A further source of nonlinearity in this region stems from the rigid backing. It is hypothesized that the interface between the backing and the arch barrel has cracked and, as such, connectivity between these components is only possible in compression. Therefore, neither FE models with or without the rigid backing would represent the true behaviour of this interface at all points in time. As a train passes overhead, the rigid backing would rotate about the skewback as the adjacent arch barrels spread and contract in sequence. The rigid backing remains in contact with one of its adjacent barrels at a time and, when connectivity exists, FE model 4 will capture the interaction between the barrel and rigid backing. However, as soon as the two regions separate, behaviour might more closely resemble model 3, in which the rigid backing is not included.

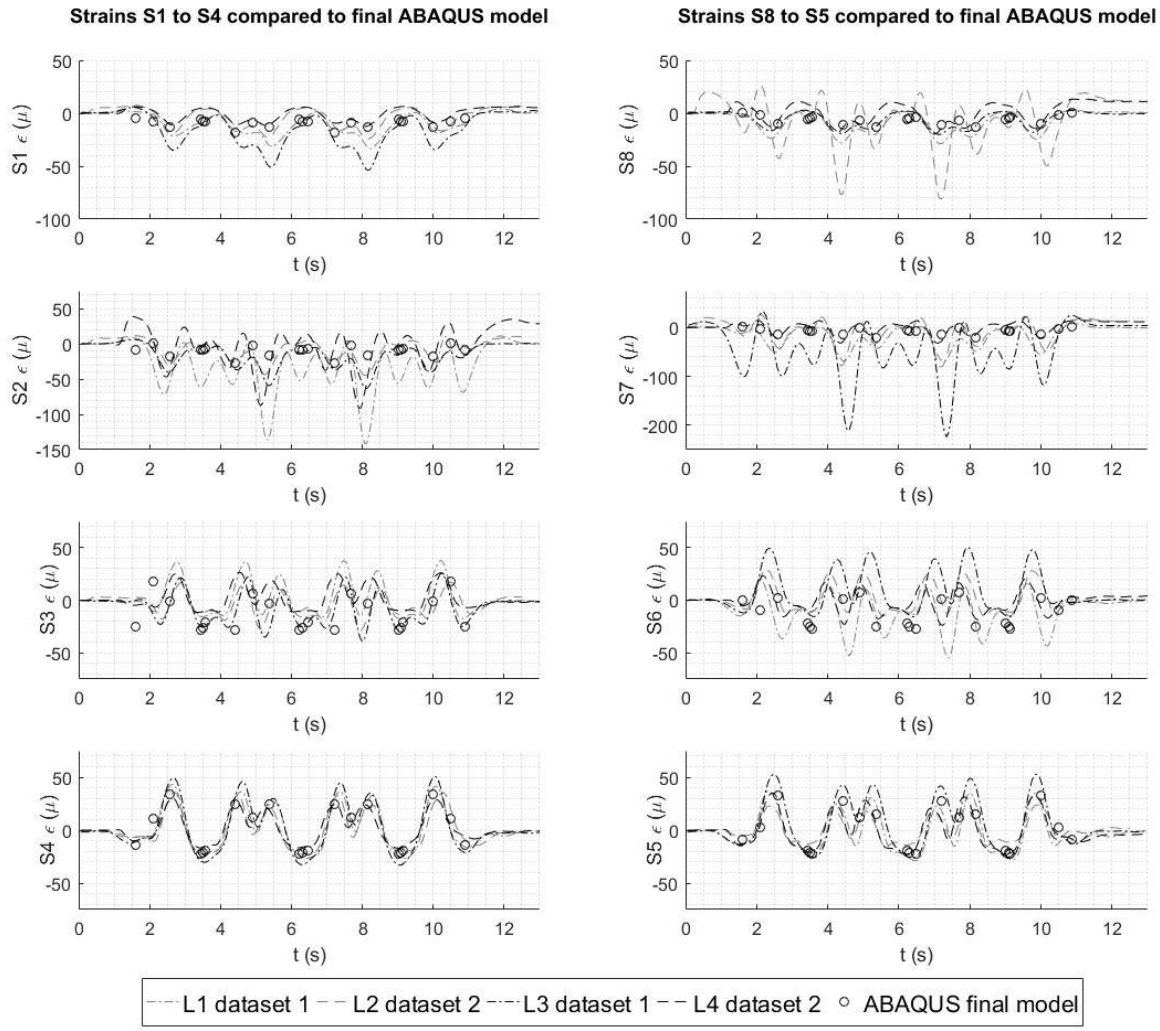

Figure 10: Comparisons of local strain response at locations S1 to S8, for the final FE model and the real viaduct.

5.4 Recommendations

From this study, it is clear that the full impact of damage cannot be observed in standard global response parameters, such as the crown vertical displacement or the pier-to-pier span opening; damage is only seen as an increase in the magnitude of the response. Both of these measurements are taken at points on the structure which are far enough removed from common locations of damage that there is no significant change in the pattern of the measured response.

In order to tell the severity of damage from global response characteristics, it is therefore necessary to have knowledge of the magnitude of this response before the damage took place. If a monitoring scheme was not in place prior to the damage occurring, computational analysis may be useful to assess the undamaged condition of the structure. To do so accurately requires detailed knowledge of the structural geometry and material properties, which may be impractical to obtain.

However, since the pattern of the local response is significantly altered by damage and the subsequent onset of nonlinear behaviour, another option could be to change the location at which measurements are taken. For example, since typical damage suffered by masonry arch bridges might include transverse cracks close to the vertical level of any rigid backing, one potential location might be the third-point of the span, instead of the crown. Strain measure-

ments taken at this location would not only give the current magnitude of response but also the current pattern, which may well be expected to change as nonlinearities develop and begin to dominate the local structural behaviour.

6 CONCLUSIONS

This paper has summarised the monitoring installation at Marsh Lane viaduct, which was able to ascertain the complex behaviour of this structure under its service loads [1]. It then goes on to present the findings of a finite element investigation which sought to compare the viaduct monitoring data against a linear elastic baseline response, corresponding to the undamaged behaviour. Although uncertainties regarding input parameters mean that the models cannot claim to be a perfect representation of this specific viaduct, some conclusions can still be drawn regarding the possibilities of simplified serviceability analysis.

First, relative stiffness contributions to the serviceability response have been presented for the key structural components of a masonry arch viaduct. Some of these components are sometimes omitted from standard analysis; the results here confirm that this may lead to significant underestimation of the true structural performance.

The comparison between FE models and monitoring data looks separately at global and local response parameters. The results indicate that the pattern of the global response parameters has not drastically changed, even though damage to the viaduct means that some of its current behaviour must be nonlinear. However, on the local scale the damage does have an effect, sometimes profoundly so, on the pattern of the response. It can lead to significant departures from the linear elastic deformation mode, even though the damage may not be observable in the global response as more than an increase in magnitude, which might initially be relatively minor.

This is important, because standard UK practice is to monitor the crown vertical displacement of bridges deemed to be at risk. It may be more useful to obtain an alternative point measurement, perhaps capturing the strain response at the third-point of the span where both the magnitude and the pattern of the response can contain useful information.

7 ACKNOWLEDGEMENTS

This research was funded by an EPSRC Doctoral Training Partnership (Grant Reference Number EP/M506485/1), and through the Cambridge Centre for Smart Infrastructure and Construction (EPSRC Grant Reference Number EP/L010917/1). In addition, the authors are grateful to Network Rail for their support.

REFERENCES

[1] M.S. Acikgoz, M.J. DeJong, C. Kechavarzi, K. Soga, Dynamic response of a damaged masonry rail viaduct: Measurement and evaluation (under review).

[2] https://www.imetrum.com/, website of Imetrum Ltd – Non-contact precision measurement, 2018.

[3] https://vimeo.com/191376460, video of “skewback rocking” taken by Bill Harvey, Bill Harvey Associates, 2018.

[4] http://www.reluis.it/index.php?option=com_mada&Itemid=160&lang=en, online masonry database (MADA), 2018.

[5] Italian Seismic Design Code (OPCM 3274/03 and further modifications), EUCENTRE, 1987.

[6] G. Gazetas, Formulas and Charts for Impedances of Surface and Embedded Foundations. *Journal of Geotechnical Engineering*, **117**(9), 1363-1381, 1992.

[7] A. Brencich, G. Cassini, D. Pera, Load Bearing Structure of Masonry Bridges. *ARCH'16: Proceedings of the 8th International Conference on Arch Bridges*, Wroclaw, Poland, 5-7 Oct 2016, 767-774.

[8] T.E. Boothby, D.E. Domalik, V.A. Dalal, Service Load Response of Masonry Arch Bridges. *Journal of Structural Engineering*, **124**(January), 17-23, 1998.

[9] P.J. Fanning, T.E. Boothby, B.J. Roberts, Longitudinal and transverse effects in masonry arch assessment. *Construction and Building Materials*, **15**(1), 51-60, 2001.